1 **SUPPLEMENTAL MATERIAL**

1.0 Experimental cross-contamination: supplemental methods and results

1.1 Rotifer clones

To test the effect of adding two different animals to one tube, we selected two bdelloid rotifer clones from our cultures. One is the clone that supplied DNA for the reference genome of *A. vaga* (Flot et al. 2013), kindly provided by K. Van Doninck in 2013. We believe it was collected originally in Italy (Mark Welch & Meselson 1998). We call this clone "*A. vaga* (AD008)" or "*A. vaga* (genome)". The second clone was isolated from *Brachythecium rutabulum* (Hedwig), growing on *Quercus* sp. at Silwood Park, Ascot, UK (51° 24' 32.06" N 0° 38' 41.71" W), and kept in continuous culture since 2012-01-09. We call this clone "*A.* sp. (AD006)". According to Debortoli et al. (2016), the most frequent signatures of "interspecific recombination" were observed between the *A. vaga* "cryptic species" A and E, and between C and E. These pairs of species share 86.1% and 86.4% sequence identity respectively at the mtCO1 marker.The identity between AD008 and AD006 at the mtCO1 marker is 86.5%, and thus commensurate with the species pairs involved in potential cross-contamination. Both clones were cultured using methods described previously (Wilson & Sherman 2010). Every two to three weeks, bdelloid populations were moved to fresh dishes of sterile distilled water over Czapek-Dox 0% agar (Barron 2004). Cultures were fed with a standardised inoculum of *Escherichia coli* (OP50), and *Saccharomyces cerevisiae* (S288c).

1.2 Design and replication

We prepared 12 tubes, divided into three groups and replicated as shown in Table S1. Biological replicates refer to different tubes, technical replicates refer to repeated PCR and sequencing using the same tube of template DNA. For each of the groups (1X6, 1X8, 2X6-8), one biological replicate was selected for technical triplication. For the 2X6-8 group, a further two biological replicates were selected for technical duplication.

1.3 Rotifer isolation

For our experiment, it was critical to be certain of the exact number of rotifers in each tube. The methods and citations provided by Debortoli et al. (2016) do not describe the technique used to isolate animals. We requested a protocol from the authors, and were given the following summary:

"Our procedure is simple, we collect the lichen/grass patch and put it in Spa® water overnight. The next day, we isolate the individuals identified as *A. vaga* by pipetting and washing them in clean water drops (serial dilutions). We then carefully checked under the binocular each tube to make sure that only one individual was present." (N. Debortoli and K. Van Doninck, pers. comm.)

This description raised some technical concerns for us. Prior to 2014, we had employed a similar procedure, but we found that pipettes were unsuitable for systematic isolation of individuals from nature, and that quality control procedures requiring visual inspection of Eppendorf tubes were inherently unreliable. Bdelloid rotifers are tiny, transparent and often rest motionless and invisible under the distortion of a meniscus or against the plastic base of a tube. They frequently stick inside pipette tips and are very difficult to dislodge or even to see. This leads to lost time and plasticware, and more seriously, to loss of specimens and bias in the subset of animals that successfully pass through the protocol. We occasionally experienced contamination via the following events. An individual is serially washed and deposited into a tube by pipette. The tube is carefully checked under the binocular microscope, but no animal is detected. It is assumed that the specimen was stuck in the pipette tip, but this cannot be directly verified. The tip is changed, and a second rotifer is serially washed and placed in the tube. This time, when the tube is carefully checked, a rotifer is visually confirmed, and the tube is sealed for DNA extraction. In fact, the first animal also entered the tube, but was hidden under the meniscus or on the bottom; thus, two rotifers now share one tube. This is not a particular problem when isolating animals from a clonal culture, but becomes a critical technical issue when isolating genetically different animals from nature. Opportunities for contamination increase when large numbers of animals must be isolated.

To address these problems, we now use a needle-based protocol when isolating individuals. This protocol is described in Additional File 1, and was used to prepare experimentally cross-contaminated samples. Into each of the 12 experimental tubes, 8µL of sterile Milli-Q water was pipetted. To each tube in groups 1X6 and 2X6-8, the needle protocol was used to move a single rotifer from a stock culture of *A.* sp. (AD006), via a wash droplet of 1mL sterile Milli-Q water. To each tube in groups 1X8 and 2X6-8, a single rotifer was moved from a stock culture belonging to *A. vaga* (AD008). The tubes in group 2X6-8 therefore contained two rotifers, one from each species.

1.4 DNA extraction and sequencing

We extracted DNA from the samples and amplified the mitochondrial cytochrome oxidase I (mtCO1) marker by PCR using the methods described by Debortoli et al. (2016). We used the same primers (LCO1 and HCO1; Folmer et al. 1994) at the same concentrations, and the same concentration of template in the same reaction volume (25µL). Amplifications were performed using GE Healthcare illustraTM PuReTaq Ready-To-Go PCR Beads. PCR products were purified, and sequenced in both directions with the same primers using an ABI 3730xl DNA Analyzer (Applied Biosystems), via a commercial Sanger sequencing service (Macrogen Europe, Amsterdam, The Netherlands).

1.5 Replicability of results

Technical replicates within the 2X6-8 group were concordant and the same clone always dominated the amplicon pool, but biological replicates showed different dominant clones (Table S2). For three samples, *A. vaga* (AD008) supplied the majority haplotype (99.5%, 99.3% and 99.6% of bases called); for the other three samples, *A.* sp. (AD006) was in the majority (99.6%, 99.7%, 97.9%). Concordance among technical replicates suggests that small differences in efficiency of lysis or DNA extraction are at least as important as differences during PCR in determining which of the genomes is amplified. Consequently, it may not be surprising to see a consistent majority sequence when amplifying repeatedly from the same sample, even if it contained multiple animals. The discordance among biological replicates suggests that the direction of the bias may be inconsistent between samples, even when the same two species are involved.

Figure 1 presented results from bidirectional pairs of sequencing chromatograms for Samples 1X6_01a and 2X6-8_03a, where *A.* sp. (AD006) was in the majority and *A. vaga* (AD008) in the minority. To check robustness in the reciprocal case, we repeated the analysis for Samples 1X8_02c and 2X6-8-05a, where *A. vaga* (AD008) was in the majority. The outcomes were as expected (Figure S1). Again, the minority peaks for AD008 often were hidden within noise associated with polymerase slippage and other errors, but the contaminant was recovered via ConTAMPR.

2.0 Methods for chromatogram quality analysis

Sequencing chromatograms for our experimental samples were returned by Macrogen Europe in the ABIF format, which included phred quality scores (Ewing & Green 1998). Chromatogram files were provided by Debortoli et al. in the .scf file format. We used CodonCode Aligner (v. 7.0.1, CodonCode

Corporation) to assign phred quality scores to these chromatograms, which were imported for further processing in Geneious (v. 8.1.9, Biomatters Ltd, Auckland, New Zealand; Kearse et al. 2012).

Chromatograms for mtCO1 were uniformly trimmed to 605bp to avoid sequencing artefacts near the priming sites, and phred Q20 quality scores are reported for this section. The boxplots shown in Figures 4 and 5 were produced using R (v. 3.3.1, R Core Team) with the default setting for whisker length, and annotated manually. The two distributions were plotted separately in Figure 5 because they were statistically different. Owing to obvious outliers, distributions of quality scores for the chromatograms of Debortoli et al. (2016) were not assumed to be normal, and were compared using the Mann-Whitney test, implemented in R through the "wilcox.test" function. The equivalent distributions for our new data were approximately normal, but the difference between groups was not significant whether analysed using a parametric (N=38, t=1.13, P = 0.26) or nonparametric approach (N=38, Mann-Whitney W=234, P=0.1186).

The 28S ribosomal marker was amplified by Debortoli et al. in four overlapping fragments. This locus is highly conserved among even distantly related species. We restricted all our analyses to the first fragment, amplified with the primers 28S0FCT and 28S1RCT (Debortoli et al. 2016). Among the six *Adineta* species reported by Debortoli et al (2016), this fragment has 70 variable sites in 700bp (10%), whereas only 24 variable sites are found in the remaining 1610bp (1.5%). We trimmed chromatograms to a uniform length of 659bp (28S0FCT) or 666bp (28S1RCT) and calculated phred quality scores for this informative region. We focused on the Q40 phred score because the overall quality of 28S chromatograms was higher than for mtCO1; we suggest that the whole-genome amplification step tended to increase the representation of a single template and reduced or eliminated competing signals, especially after further PCR.

The distribution of 28S quality scores was shifted significantly lower for samples where HGT was claimed (Figure 5, Mann-Whitney Test: N=122, W=373.5, P=0.015). Both the median and second-highest quartile of the "HGT" samples fall within the second-lowest quartile of the "non-HGT" samples. The HGT group also had significantly more files with scores below 80% (Fisher's Exact Test, 4 in 12 versus 2 in 121, P=0.0006**;** or if we treat paired chromatograms from the same sample as non-independent, 2 in 6 versus 1 in 60, P=0.019).

No attempt was made to assess quality scores for EPIC25 chromatograms, because even if DNA all comes from a single animal, these amplicons represent a pair of homologous intronic regions that

frequently are separated by at least one insertion-deletion polymorphism (indel), which means two sets of peaks are superimposed out-of-phase in some regions (Debortoli et al. 2016), rendering quality scores uninformative.

3.0 Contingency table analysis of minority peak ranks (ConTAMPR)

3.1 Multiple sequence alignments

The sequences of all haplotypes delimited by Debortoli et al. (2016) were retrieved from GenBank (KU860573–KU861170), along with relevant sequences for the *A. vaga* reference clone (GQ398061; JX184001), *A. ricciae* (EF173187; KM043216) and *A.* sp. AD006 (KM043183). Multiple alignment of chromatograms and candidate sequences was performed using MAFFT v. 7.017 (Katoh et al. 2009), implemented in Geneious using the MAFFT plugin (v. 1.3.3). For some sequences, particularly mtCO1, this algorithm alone was sufficient to bring peaks for the majority and putative minority sequences into alignment with the reference haplotypes. This is because there are no indels between species for the mtCO1 marker, so peaks corresponding to amplicons from different templates are superimposed ('in-phase'), though we typically saw slight displacement of minority peaks by less than a base-width in one direction or another relative to the majority peak. This is illustrated in Additional File 2, using annotated screenshots from the visual interface of Geneious.

For 28S rDNA, a multiple alignment of all unique sequences for *A. vaga* Species A-F revealed three indels of 1-2bp within a single 100bp region of the focal first fragment (Figure S2). This occasionally created challenges in testing whether two sequences from different species were present in an amplicon population. For instance, Sample B14 was predicted to include haplotypes from Species A and E. There is a single 1bp indel between these species (at position 134 in Figure S2), which means the minority peaks in a forward chromatogram are predicted to run approximately in-phase with the majority peaks until the indel, then become misaligned by 1bp, whereas the minority peaks in a reverse chromatogram will show the opposite pattern. The contaminant might thus be mistaken for a polymerase slippage artefact (Mullis et al. 1994). To analyse such a pattern, it is necessary to manually shift the alignment of each chromatogram by 1bp around the indel, which means the majority peaks are out of phase with the aligned majority haplotype for part of its length. This alignment shift is illustrated in Additional File 3. For clarity, we point out every base corresponding to the minority Species E haplotype in both directions. The pattern of multiple peaks changes

exactly as predicted at the site of the 1bp indel between Species A and Species E, which thus represents further, sequence-independent evidence for the additional haplotype.

EPIC25 is a highly variable intronic marker with multiple indels of up to 12bp within and 23bp between *A. vaga* Species A-F. Superimposed sequences from different species are therefore displaced even further and more frequently than at 28S, which makes it challenging to align even one candidate haplotype to the minority peaks. Multiple manual adjustments to an initial MAFFT alignment were necessary to follow the minority haplotype after each indel. It would not be feasible to attempt to align haplotypes from more than two candidate species at once against these chromatograms, since the peaks and variable sites would almost never be predicted to coincide with both candidates. However, it was not necessary to align every species individually to test for the EPIC25 sequences listed in Table 1, because the predicted matches were so clear and the alignment constraints made a match to any alternative haplotype so improbable. Additional File 4 illustrates the alignment shifts necessary to follow a minority Species A haplotype running alongside a Species E haplotype with at least 5 dispersed indels of varying lengths. Each peak we interpret as corresponding to the minority haplotype is individually highlighted.

3.2 Peak rank assignments

After bidirectional pairs of chromatograms had been aligned with candidate sequences, we manually scored the relative heights of minority fluorescence peaks at each site where a candidate sequence differed from the majority haplotype. We examined the trace lines corresponding to the remaining three nucleotides. Where these formed clear peaks, we assigned ranks 2, 3 and 4 based on their relative heights, and recorded the rank corresponding to the required base for each candidate sequence. The absolute heights were not considered, because we determined experimentally that peaks corresponding to a known second animal may be very small, inconsistent or even absent (Figure 1). Where two peaks appeared equal in height, we increased the magnification of the chromatogram using the Geneious interface until a difference, however small, became clear. If no such difference was apparent, the available ranks were randomly assigned to the two peaks.

When the minority sequence was 1bp out of phase with the majority haplotype, minority bases sometimes did not correspond to distinct peaks, but produced either a trailing or a leading 'tail' attached to the preceding or succeeding peak. In these cases, there was usually a local maximum or at least an inflection point which we took as the height of the peak. If a base did not correspond to a

clear peak, local maximum or inflection point, we estimated the mean relative heights of the trace lines at that site, regardless of shape. Where the trace line for a nucleotide showed absolutely no signal at a site, we recorded rank "5" to indicate this feature, but treated it as a fourth-ranked peak call for the purpose of analysis. Very rarely, the trace lines for two nucleotides both were flat, with no fluorescence signal. In these cases, the two missing nucleotides were each annotated as "6", and these were later split equally between ranks 3 and 4 for analysis.

At a locus like mtCO1, where all sequences are 'in-phase', the majority peak by definition cannot be called to represent a minority variant. However, Additional Files 3 and 4 illustrate a complication that occurs when majority and minority peaks are not aligned in phase, as at 28S and EPIC25. Sometimes, the expected minority peak at a variable site will happen to match the out-of-phase majority peak. This is a pure coincidence, but it prevents an assessment of how high the predicted secondary peak would have been otherwise, and it is not trivial to predict how often this is expected to happen under the null hypothesis. Where the "minority" haplotype happened to match a shifted majority peak, we recorded "1" as the rank, and we took a conservative approach and simply excluded all of these first-ranked "minority" calls from contingency analyses.

3.3 Statistical analysis of contingency tables

If minority peaks are a consequence of noise, non-rotifer contaminants, polymerase slippage or other sequencing artefacts, then all else being equal we predicted that the peak ranks corresponding to any control rotifer sequence would not differ significantly from an equal distribution (i.e. a 1:1:1 ratio for second, third and fourth-ranked peaks). We validated this prediction using chromatograms from our "1X" experimental groups (e.g. Figure S1). Alternatively, if a second haplotype is present, the set of peaks corresponding to that haplotype ought to differ significantly from the null distribution, showing a significant bias in favor of second- rather than third-ranked peaks, and third- rather than fourth-ranked peaks. For each candidate haplotype, we tested whether the peak rank distribution differed significantly from the null hypothesis of a 1:1:1 ratio, using Pearson's Chi-squared test for count data (Agresti 2007), implemented in R via the "chisq.test" function.

In many cases, more than one alternative sequence produced a significant deviation from the null distribution. This is expected, because at many variable sites an alternative base is shared by more than one rotifer species; therefore, the true matching sequence will 'drag up' the rank distribution of species that share bases. For example, in Figure 1B, the *A. ricciae* control sequence deviates from the

null expectation (χ^2=64.9, d.f. =2, P = 8.07 x 10^{-15}), but only because it shares some variants with the true contaminant: *A.* sp. (AD006). Excluding these shared sites abolishes the fit (χ^2= 3.2, d.f. = 2, P=0.202). Figure 3 further illustrates the effect of relatedness. To distinguish the primary match, we compared the degree of fit not only against the null distribution, but among different candidate species. We typically used the Chi-square test of independence for a 3 x n contingency table, where n is the number of candidate species or haplotypes. If the initial table included cell counts too small to meet the assumptions of the test, two or more control species were pooled. Table 1 indicates the species or haplotypes that were used for each comparison; distributions that were pooled are indicated with "&". In some cases, further pairwise contrasts are reported in the text. To correct for the problem of multiple comparisons, α was adjusted using the Bonferroni correction, but all hypothesis tests remained significant even using this highly conservative approach.

4.0 Neighbor-joining phylogeny

The phylogenetic tree in Figure 3 was constructed using the neighbor-joining method implemented in the Geneious Tree Builder tool, with the default settings and 100 bootstrap replicates.

5.0 Supplemental results for samples claimed to be cases of interspecific DNA transfer

Analysis of chromatograms for the six apparently incongruent samples indicated that some contained DNA from more than one animal, while others contained the predicted "original copies" of genes that had supposedly been replaced via interspecific horizontal genetic transfer. The results are summarised in Table 1, and this section discusses each of the samples in greater detail.

5.1 Sample B11

To test the hypothesis of cross-contamination for Sample B11, it was necessary to predict which 28S and mtCO1 haplotypes a putative second animal from Species E might have. We consulted Table S3 of Debortoli et al. (2016), and found that only Individual 81 [E] shares all the Species E haplotypes that feature incongruently in Sample B11. We therefore aligned the B11 chromatograms to the haplotypes of that individual: Hap31 [E] at mtCO1, and Hap13 [E] at 28S. The choice of control haplotypes to represent each of the other species (Figure 2) was random. Peak rank distributions for the six control species were statistically indistinguishable from each other (χ^2=6.66, d.f. = 10, P = 0.76), and only differed from the null expectation because each happened to share some bases with

Hap31 [E]. For example, if we exclude polymorphisms *A. ricciae* shares with Hap31 [E], it no longer differs from an equal ratio of second, third and fourth peaks (30:40:26; χ^2=3.25, d.f. = 2, P = 0.197).

Although ConTAMPR revealed additional mtCO1 and 28S haplotypes for Sample B11 (Figure 2; Table 1; Additional File 2), the corresponding chromatograms are not obvious outliers in terms of phred quality scores (Figure 4; Figure 5). At 28S, for instance, both chromatograms for Sample B11 lie within the interquartile range for samples where no HGT is claimed. This is consistent with the results of our experiments: even when multiple animals are present, we do not necessarily see obvious differences in chromatogram quality, since minority peaks may be very small, or absent.

If Sample B11 contained two animals, it is interesting that the majority haplotypes for mtCO1 and 28S were from Species A, whereas those at EPIC25, EPIC63 and Nu1054 were from Species E. This may simply reflect the chance outcome of two consecutive nonlinear amplifications (WGA and PCR). However, the guanine-cytosine (GC) content of the Species A haplotypes expected at EPIC25, EPIC63 and Nu1054 is much higher than the corresponding Species E haplotypes that Debortoli et al. recovered (+17.7%, +13.6%, +21.2% respectively), whereas GC differences were much lower at mtCO1 and 28S (+1.9%). The whole-genome amplification kit used by Debortoli et al. has been found to show a bias in favor of templates with lower GC content (Han et al. 2012), and multi-template PCR also is sensitive to this parameter (Polz & Cavanaugh 1998). Substantial differences in GC content may have helped to skew amplification of the competing haplotypes, effectively masking Species A at EPIC25, EPIC63 and Nu1054. At mtCO1 and 28S, GC was not substantially different, and the identities of both animals were recovered via ConTAMPR, though their representation was far from equal. Owing to effects like this, absence of evidence is not evidence of absence when considering amplicons from potentially contaminated samples. Even if two animals are present, one may be masked by the other at certain loci or in certain amplifications. It is very difficult to exclude the hypothesis of contamination on the basis of apparently clean chromatograms, but it is immediately telling to discover an extra haplotype.

5.2 Sample B22

The predicted donor of the incongruent EPIC25 haplotype in "Individual 58" was Species E. In animals of this species, Table S3 of Debortoli et al. (2016) shows that EPIC25 Hap37 [E] occurs with mtCO1 Hap29 [E] and 28S Hap16 [E]. For ConTAMPR, we therefore aligned the B22 mtCO1 and 28S chromatograms against these candidates, along with control sequences from other species. Again,

we found evidence for the predicted haplotypes (Figure S3, Figure S4). The extra 28S haplotype in Sample B22 was sufficiently prominent that the phred quality scores for these chromatograms fell outside the range of values for samples where no HGT was claimed (Figure 5).

We examined chromatograms for Sample B22 at the EPIC25 marker itself, where the authors reported a single, incongruent haplotype: Hap37 [E]. We did not find evidence for an expected 'native' Species C sequence. We suggest this haplotype was lost either during PCR or WGA, perhaps in part because its GC content would have been approximately 22% higher than Hap37 [E].

The authors characterised "Individual 58" as "homozygous" at EPIC25. However, it is clear from the data that a second Species E haplotype also was present in Sample B22. The trace files show hundreds of double and triple peaks of comparable heights. As discussed above, these represent two genomic homologs, running slightly out of phase following an indel, and with triple peaks indicating further single nucleotide polymorphisms (SNPs) between them. There are at least 7 SNPs between Hap37 [E] and the other haplotype in Sample B22, along with the indels. Many of these appear to correspond to standing polymorphisms shared by other animals in the Species E population (Figure S5). The presence of two quite divergent "transferred" haplotypes in a putative recipient individual is important. It is not consistent with the HGT scenario posited by Debortoli et al. (2016), in which interspecific recombination replaced the original DNA at one site, and "gene conversion promptly copied the integrated DNA on its homologous region". That would produce two identical haplotypes in the recipient. It would not preserve various SNPs and indels found in a "heterozygous" donor. On the other hand, this pattern is predicted if the haplotypes arose from a contaminating animal belonging to Species E, which had heterozygous combinations at EPIC25 similar to those seen in Individuals 81 (Hprim14a/b) and 78 (B39a/b). This is an independent line of evidence for the conclusions supported by ConTAMPR at 28S and mtCO1.

5.3 Sample B39

Debortoli et al. (2016) interpreted Sample B39 as Individual 66 [E]. A Species E mtCO1 haplotype had been replaced, in their view, by one imported from Species C. An alternative hypothesis is that Sample B39 was cross-contaminated with some DNA from Species C, which happened to be amplified by the mtCO1 primers instead of the native sequence. This hypothesis predicts a Species E haplotype congruent with the other loci among the minority mtCO1 amplicons. Specifically, Table S3 of Debortoli et al. (2016) indicates that Individual 66 ought to have mtCO1 Hap31 [E], as seen in

Individual 81. Like Individual 66, that animal had Hap16 [E] at 28S, Hap16 [E] at EPIC63, Hap19 [E] at Nu1054 and Hap30 [E] at EPIC25. No other individual had such a combination.

We used ConTAMPR to test whether minority peaks might correspond to Species E rather than any other species, and also to Hap31 [E] rather than any other Species E mtCO1 haplotype. We aligned B39 chromatograms not only to other *Adineta* species, but to seven diverse haplotypes from Species E. We found strong and specific evidence for the 'missing' native mtCO1 haplotype predicted for Individual 66 (Figure S6). This result brings all five loci into concordance without the need to invoke interspecific horizontal genetic transfer or transformation of mtDNA, which is problematic in itself (Larosa & Remacle 2013). The only incongruence in Sample B39 is the presence of mtCO1 Hap 10 [C] among the amplicons. We attribute this either to chance amplification from loose Species C mtDNA associated with the surface or gut of Individual 66, or to a second animal whose nuclear sequences were dropped or outcompeted during WGA or PCR, as seen with samples B11 and B22.

5.4 Samples B14 and B3B1

For samples B14 and B3B1, the minority peaks in mtCO1 chromatograms were a significantly better match to several other bdelloid mtCO1 haplotypes than the null expectation. This is consistent with the presence of additional mtCO1 sequences, and therefore DNA from additional animals in these samples (Figure S7). However, the peak rank distributions for several candidate species could not be distinguished statistically when compared with each other.

Looking at other loci, we noticed that B14 and B3B1 were the only samples to show unambiguous evidence of haplotypes originating from at least three different species (in each case, A, C and E; Table 1). We guessed that we were unable to identify a single consistent secondary sequence at mtCO1 because three animals from quite different species had contributed DNA to these samples. This hypothesis was supported by the fact that mtCO1 chromatograms from these two samples were extreme outliers in quality (Figure 4). The presence of DNA from three animals would explain why additional mtCO1 haplotypes cannot be narrowed down to a single candidate. Relative to the subtle minority peaks produced when we added just one extra animal (Figure 1B), the noise is such that almost any *Adineta* haplotype could be present. The hypothesis of "interspecific horizontal genetic transfers" supplies no obvious explanation for the unusual features of the mtCO1 amplicons obtained from these particular samples.

For Sample B14, we found evidence of an additional haplotype at 28S, consistent with Species E and a better match by a significant margin than more distantly related species (Figure S8). This suggests that one of the additional animals belonged to Species E, which would explain the incongruent Species E haplotypes Debortoli et al. (2016) found at EPIC63 (Table 1). Peaks corresponding to this additional haplotype also explain the unusually low phred quality scores for the 28S chromatograms for Sample B14 (Figure 5). These peaks are annotated fully in Additional File 3. The absolute heights of secondary peaks were often very low, as we saw at mtCO1 when we deliberately added two animals. At 28S, this may reflect preferential nonlinear amplification of one haplotype during both WGA and PCR. This would explain why some of the other contaminated samples (e.g. B11) did not show obviously anomalous 28S quality scores, or sometimes any detectable second 28S haplotype (e.g. B3B1). Conversely, no horizontal exchange was claimed for Sample A3B1 ("Individual 56" [C]), yet it was another clear outlier in Figure 5. We were not provided with mtCO1 or EPIC25 chromatograms for Sample A3B1, but the evidence from 28S suggests that DNA from a second animal was present. Perhaps no interspecific recombination was claimed because the same animal's sequence happened to be in the majority at all loci. The true incidence of interspecific cross-contamination is likely to be higher than the six samples where incongruence was noted.

For Sample B14, we found evidence of an additional EPIC25 haplotype consistent with Species E, even though two EPIC25 haplotypes from Species C had already been reported by Debortoli et al. The match was significantly better than the null expectation (χ^2=11.18, d.f. = 2, P = 0.00374). The presence of a third EPIC25 haplotype in a single sample is suggestive regardless of its identity, since no single animal in the study of Debortoli et al. had more than two copies of this marker. Only one chromatogram was provided (for the primer EPIC25F), and without the guidance of bidirectional reads for this variable and indel-rich marker, we did not attempt to align other species.

Debortoli et al. reported just one EPIC25 haplotype for Sample B3B1, matching Species E. However, we found evidence of at least one and possibly two further EPIC25 haplotypes uniquely matching Species C (Table 1). The fit was significantly better than the null expectation (χ^2=108.44, d.f. = 2, P < 2.2×10^{-16}); indeed, given the indel issues discussed above, no other species could be aligned to the minority peaks. The model of interspecific recombination and gene conversion offered by Debortoli et al. has difficulty accommodating two different non-native sequences at one locus, in addition to the more serious obstacles we report elsewhere. The 'native' EPIC25 sequence we would predict for Species A was not recovered; we suggest it was dropped during WGA or PCR. At the noisy mtCO1 locus, Species C again showed the strongest evidence of a fit to minority peaks (Figure S7, χ^2=12.9,

d.f. = 2, P = 0.00158), though the fit to Species E also differed significantly from the null expectation (χ^2=7.35, d.f. = 2, P = 0.0254). This evidence points to Species C as one of the contaminants. Our interpretation is that Sample B3B1 contained animals or loose DNA belonging to Species A, C and E.

5.5 Sample D14

Debortoli et al. (2016) interpreted Sample D14 as "Individual 5", and inferred that a Species A EPIC25 sequence had been replaced by Hap10 from Species C. If the incongruent sequence instead came from a second animal or contaminant DNA from Species C, then a native Species A sequence is expected among the amplicons. Table S3 of Debortoli et al. (2016) predicts either Hap1 or Hap4 [A]. In the chromatograms, Hap10 [C] is in the majority, but in both directions a second sequence with peaks of almost equal height runs several base pairs out of phase, as expected if indels are present. It corresponds exactly to Hap4 [A], with a specific number of GAA tandem repeats to distinguish it from Hap1 [A]. Additional File 4 shows these aligned chromatograms, pointing out peaks matching the second sequence, and highlighting sites where it differs from the Hap 10 [C] interpretation. It was not necessary to attempt to align all the other *Adineta* species to these chromatograms and compare peak heights, as EPIC25 is so variable that no other species would match. Almost all base calls for Hap4 [A] use either first or second-ranked peaks, and no fourth-ranked peaks are needed at all. The probability of this happening by chance is negligible (χ^2=75.97, d.f. = 2, P < 2.2 x 10^{-16}). The most parsimonious interpretation is that Individual 5 had concordant Species A haplotypes at all loci in the expected combinations, but its sample tube (D14) was contaminated by DNA from Species C, bearing an EPIC25 haplotype that was amplified by WGA and PCR along with the native haplotype.

As discussed in the text, Debortoli and colleagues supplied two separate bidirectional pairs of EPIC25 chromatograms for Sample D14. Each pair represented an independent PCR amplification from the same DNA sample following WGA (N. Debortoli, pers. comm.). In one chromatogram pair, discussed above, the expected Species A sequence was unambiguous. Importantly, however, this native sequence was absent from the second pair of chromatograms, even as minor secondary peaks (Additional File 4). Even on close scrutiny, only the incongruent sequence from Species C was visible. Clearly, the DNA in the template tube had not changed from one PCR to the next; therefore, the inconsistency arose from complete loss of a haplotype during the dynamics of multi-template PCR.

6.0 Pairwise genetic identity and microhomology analyses

441 **6.1 Pairwise marker alignments to determine homology between species**

442

443 To determine pairwise homology between sequences involved in “interspecific recombination”, we
444 aligned the putative donor and recipient haplotypes in each case as described above using the
445 MAFFT v. 7.017 algorithm (Katoh et al. 2009), implemented via the Geneious plugin (v. 1.3.3) with
446 default settings. We then recorded the pairwise identity for each alignment and the GC content of
447 each sequence, as reported in the Geneious "Statistics" interface.

448

449 **6.2 Validation of pairwise homology calculations for wider genomic regions**

450

451 The genetic distances in Table 2 are estimated for short (<1kb) markers that Debortoli et al. (2016)
452 selected for easy amplification. However, horizontal transfer events are claimed to extend several
453 kilobases beyond the markers they encompass (Figure 5 of Debortoli et al. 2016). We considered
454 the possibility that genomic regions beyond the focal markers might show substantially greater
455 sequence homology between species, thereby decreasing the mechanistic implausibility of HGT. For
456 example, the EPIC25 marker (ca. 400bp) spans the first intron of a gene approximately 4.3kb long,
457 encoding a product with similarity to the vertebrate metastasis suppressor protein 1 (MTSS1). In the
458 *A. vaga* reference genome (Flot et al. 2013), the next-closest gene is approximately 2kb from the
459 marker in a 5' direction, and encodes a product with similarity to vertebrate trifunctional enzyme
460 subunit beta (HADBH). Because introns are often highly variable, pairwise identity at the EPIC25
461 marker might underestimate the homology between two species for the shared genes in this region.

462

463 We tested this hypothesis for the "interspecific recombination" event inferred from Individual 58
464 (Sample B22), in which EPIC25 Hap10 [C] was putatively replaced by Hap37 [E]. At the marker itself,
465 these haplotypes only shared 68.4% genetic identity. We wanted to determine whether the value
466 might be higher if we considered the wider region. While investigating putative intraspecific
467 exchange, Debortoli et al. (2016) sequenced a longer (10.8kb) region surrounding EPIC25 Hap10 for
468 two other individuals in Species C (42 and 51). The region containing the genes *MTSS1* and *HADBH*
469 was syntenic with the *A. vaga* reference genome. To determine homology, we would ideally align
470 this extended region with its counterpart in Species E, but no sequenced genome for E is available.
471 However, the reference genome clone of *A. vaga* ("AD008") happens to be very closely related to
472 Species E (Figure 3). In fact, homology to Hap10 [C] at the EPIC25 marker is identical (68.4%) for
473 Hap37 [E] and AD008. We compared the equivalent identities at all five available loci, and in each
474 case, the homology to Species C was nearly identical for Species E and the *A. vaga* reference genome

(Table S3). This coincidence enabled us to use the *A. vaga* reference genome as a surrogate for Species E, with some confidence that the results would reflect the relationship to Species C.

We aligned the sequenced EPIC25 region from Individual 42 [C] (GenBank: KU861136.1) against the matching region from the reference genome (Assembly GCA_000513175.1) using MAFFT as implemented in Geneious, with default settings. For clarity, we delineated a focal region from the stop codon of *MTSS1* to the stop codon of *HADBH* (8949bp, approximately centred on EPIC25). This included exons and introns from both complete genes, and the intergenic region. We then measured the pairwise identity between the species for a variety of subregions (Table S4).

The homology between these species for the whole region is 62.3%, which is less than the estimate based on the EPIC25 marker. The intergenic region is very divergent (52.4%), but even if we only compare genes, the values are either lower than the estimate from the EPIC25 marker (for *HADBH*), or identical to it (for *MTSS1*). Thus, we can reject the hypothesis that the marker-based identities in Table 2 underestimate the homology between species for broader genomic regions. The distances involved would remain incompatible with interspecific recombination even if we only looked at discontiguous exons, whose identity was 75.1% for *MTSS1*. This is nearly the same as the mean identity between independently evolving ohnologs in the reference genome (74.8%, Flot et al. 2013).

6.3 Methods for microhomology analysis

Mechanisms of interspecific recombination based on overall homology seem to be excluded for the sequence pairs we considered, which have equal or lower identities than independently evolving ohnologs within the same genomes. However, we also considered alternative mechanisms with less stringent identity requirements than HR (N. Debortoli, J.-F. Flot, K. Van Doninck, pers. comm). One example is homology-facilitated illegitimate recombination (HFID), in which "single regions of high nucleotide-sequence similarity (~200 bp in length)...initiate recombination events that lead to the additive integration of >1000-bp-long heterologous DNA fragments" (Thomas & Nielsen 2005). Another is microhomology-mediated end joining (MMEJ), whose "foremost distinguishing property... is the use of 5-25bp microhomologous sequences during the alignment of broken ends before joining" (McVey & Lee 2008). If interspecifically transferred sequences share longer or more frequent mismatch-free blocks than genomic ohnologs (Vulić et al. 1997), then HFID or MMEJ may explain how they undergo frequent exchange while ohnologs with higher global homology evolve independently.

To test this hypothesis, we estimated the length and frequency of microhomologous blocks for genes surrounding the putative transfer seen in Sample B22, between EPIC25 Hap10 [C] and Hap37 [E]. As above, we used the genome reference clone for *A. vaga* (AD008) as a surrogate for Species E (Table S3). At every scale from 1-40bp, we compared interspecific microhomology for *MTSS1-A* and *HADBH* with intragenomic microhomology for 7650 ohnologous pairs of genes in the *A. vaga* reference genome. As an important point of comparison, we highlighted the microhomology between *MTSS1-A* and its own genomic ohnolog (*MTSS1-B*), which contains the EPIC63 marker. Debortoli et al. (2016) implicitly assume there is no exchange between these highly divergent genes, which were treated as "independent nuclear markers" and sequenced with "ohnologue-specific" primers.

Gene models for *A. vaga* were constructed using BRAKER (Hoff et al. 2015), with RNASeq as evidence (SRA accession: ERR260376; Flot et al. 2013). Collinear regions were identified using MCScanX (Wang et al. 2012), setting the maximum number of allowed gaps between collinear genes to 10. Between all pairs of collinear genes, synonymous (K_S) and nonsynonymous (K_A) divergences were calculated using the method of Nei & Gojobori (1986), implemented in BioPerl (Stajich et al. 2002). Ohnologs were defined as pairs of genes within collinear regions with $K_S \geq 0.5$ (n = 7,650). Ohnologous regions (comprising exons plus introns) were extracted and aligned using MAFFT (Katoh & Standley 2013) with default settings. Introns were included because interspecific recombination was claimed for intronic markers, and any inter-ohnolog recombination facilitated by microhomology would involve unspliced genomic DNA. Microhomology across all 7,650 alignments was calculated with a custom Perl script, using a sliding window along each alignment (sliding one base each iteration), from a size of one to 40 bp, counting any window of exact identity as a match. The number of identical blocks was scaled relative to alignment length to account for gene size, and multiplied by 1,000 to give a per-kb estimate. All scripts are available at https://github.com/reubwn/microhomology. The same method was used to measure microhomology between Species C and *A. vaga* for the alignments of *MTSS1-A* and *HADBH* discussed above. Finally, we highlighted the specific microhomology curve in *A. vaga* corresponding to the pairing between *MTSS1-A* and its ohnolog, *MTSS1-B*.

Gene copies involved in putative interspecific recombination did not share significantly more or longer blocks of microhomology than independently evolving ohnologs in the same genomes, at any scale from one to 40bp (Figure S9). At most scales they even shared less microhomology with the "donor species" than with their own ohnologs. Microhomology-based mechanisms such as MMEJ and HFIR could not facilitate distant interspecific recombination and yet fail to permit exchange

between ohnologs with even more extensive microhomology, especially as conspecific DNA fragments seem likely to be more abundant and available than heterospecific ones.

Other mechanisms of homology recognition seem even less applicable. For instance, pairing of chromosomes in early meiosis appears to be independent of recombination in some cases (Da Ines et al. 2014), but this involves chromosome-scale features such as centromeres and telomeres, which are not shared by loose DNA fragments. Pairing must still be stabilised by recombination, via sequence-dependent pathways. Another recognition mechanism involves homologous trinucleotide repeats interspersed at a specific periodicity within otherwise divergent sequences (Gladyshev & Kleckner 2016), but there is no evidence for this distinctive architecture in the putatively exchanged sequences we examined, and that pathway is not linked to recombination. It seems improbable *prima facie* that any mechanism could enable ready exchange of DNA across species boundaries, while simultaneously precluding exchange between less divergent ohnologs within the same genomes. We suggest that any argument to the contrary must bear the burden of proof.

7.0 Quantitative evaluation of evidence for "intraspecific DNA exchanges"

Using the same set of tubes, Debortoli et al. (2016) reported genetic and genomic evidence for three "haplotype trios" that they claim "can only be explained by recombination between individuals". As outlined in the main text, there is a very high probability that such patterns correspond to cross-contamination involving animals belonging to the same species. Some trios are explained even more parsimoniously "by mutations and gene conversions alone", as the authors anticipated.

7.1 Calculating the number of tubes expected to show conspecific DNA contamination

Debortoli et al. (2016) report three intraspecific "haplotype trios" at nuclear PCR markers that they interpret as "signatures of genetic exchange": two in Species A and one in Species C. Each involves a set of tubes interpreted as a trio of heterozygous individuals that appear to share alleles "in a cyclic fashion...(a||b), (b||c), and (c||a)". However, Table S5 illustrates multiple ways to generate such a pattern when tubes are cross-contaminated with DNA from two conspecific animals. As seen for “interspecific” samples, contamination may either involve genomic DNA, or amplified fragments bearing the focal locus. In the simplest case, three tubes would need to contain DNA from two animals in order to explain all three "haplotype trios" reported in the dataset. The Nu1054 trio in Species A can be completed either by Sample H3-03 (“Individual 11”) or HB01 ("Individual 13"), and

576 the latter also completes the EPIC25 trio. Contamination of these two tubes would parsimoniously
577 explain both Species A trios, with one more contamination required in Species C, for a total of three.
578
579 The number of tubes expected to contain DNA from two conspecific animals can be calculated using
580 two pieces of information. First, we need the proportion of tubes containing DNA from two animals
581 of different species. We conservatively limit this value to the six tubes identified in Table 1. The true
582 value is certainly higher, given observations about samples such as A3B1 (see Section 5.4), but
583 ConTAMPR was only applied formally to those six. Some tubes contained DNA from three different
584 animals, and thus represent two separate contamination events each, but we conservatively treat
585 these the same way as tubes with a single contamination. We also need to know the relative
586 frequencies of animals from each of the focal species in the sampled material. These are retrieved
587 from Table S2 of Debortoli et al., based on a suitably large sample (576 animals). All putative inter-
588 and intraspecific genetic exchanges involved Species A, C and E, so we can omit Species B, D and F
589 from consideration. We therefore take the heterospecific contamination rate to be 6 tubes out of
590 72, and the relative ratio of animals from Species A, C and E to be 130 : 396 : 21.
591
592 Let *t* be the probability that DNA from two individual animals was accidentally introduced to any
593 given tube. The number of contaminated tubes in the A/C/E dataset is therefore 72*t*. Let us assume
594 the two animals in each tube-sharing pair were drawn at random from the population as a whole.
595 This conservative assumption is discussed later, but it enables us to populate a table of probabilities
596 from the species ratios above (Table S6). Using this table, we can compute the expected number of
597 conspecific contamination events given that six heterospecific contamination events are observed,
598 as well as *t* itself. The calculated proportion of conspecific contamination events is 0.58206 and *t* is
599 0.199; thus, 8 tubes are expected to show conspecific contamination. The binomial distribution can
600 be applied to calculate 95% confidence intervals for this estimate (4 - 15 tubes). The probability that
601 at least three tubes show conspecific cross-contamination is 0.99267.
602
603 To estimate the probability that conspecific contamination occurred in one or more tubes assigned
604 to Species C, we used the binomial distribution and Table S6 to calculate the cumulative probability
605 that one or more of the 72 tubes experienced conspecific cross-contamination at all (0.99987). We
606 then calculated the probability that there was exactly one such event, and that this event involved
607 two animals belonging to Species A (0.00126 x 0.09728 = 0.00012). The probability of this case was
608 deducted from the initial probability (0.99987 - 0.00012 = 0.99975). The case of exactly one event
609 involving two animals from Species E ($P = 3.2 \times 10^{-6}$) can be ignored, as can the case of two or more

conspecific contamination events all involving Species A or E pairs ($P = 5.6 \times 10^{-5}$). This leaves a 99.98% probability that at least one sample interpreted as a Species C rotifer in fact contained DNA from two such animals. The most likely number of cases is 7 (95% C.I. 4-14).

These calculations make the highly conservative assumption that the species identities of any pair of rotifers in a tube are drawn randomly from the sampled population. In fact, Debortoli et al. (2016) explicitly falsify this assumption empirically in their Table S4, by demonstrating far lower odds that a pair of rotifers sampled from the same patch belong to the same molecular species versus different species. Thus, conspecific contamination is even more common than we report here. Debortoli et al. calculate an odds ratio of 11 (95% C.I. 8-16; $P < 2.2 \times 10^{-16}$), which suggests we may have dramatically underestimated the rate of conspecific cross-contamination and the total fraction of contaminated tubes (*t*). This consideration places the reliability of the 2016 dataset even further into doubt. Much of the apparent heterozygosity in *Adineta* "individuals" may well arise from two conspecific animals or their DNA sharing a sample tube. Computational phasing of chromatograms is unreliable if two or more animals (and thus four or more alleles) are present in a substantial fraction of tubes.

Conspecific contamination would be difficult to exclude empirically even using high-quality genome data, much less the "extremely fragmented" genome assemblies of Debortoli et al., where "coverage was highly heterogeneous due to the whole-genome amplification step conducted prior to library preparation". It is perhaps unsurprising "the posterior probabilities of our haplotypes reconstructed using PHASE were rather low", given that a substantial fraction of both the genomic and population reference samples are likely to contain DNA from multiple animals, and therefore more than two homologous sequences. The authors "did not detect any additional copy of the EPIC25, EPIC63, and Nu1054 markers, nor any additional 28S rDNA sequence", but this is not predicted even if conspecific contamination is present, for several reasons. First, phasing algorithms assume only two haplotypes are to be computed per individual. Second, even if more haplotypes were permitted, the Species C population lacks diversity at these loci (e.g. all sampled individuals share 28S Hap5 and/or Hap6). Third, even given higher diversity, we have shown that contamination often involves amplification of loose DNA at a single locus, with no evidence of corresponding haplotypes at other loci; thus, the scenarios in Table S5 do not predict or require three or more haplotypes at other loci.

7.2 Minimum numbers of mutations and gene conversions to explain "haplotype trios"

643 Debortoli et al. (2016) discuss two "haplotype trios" involving Species A, at the Nu1054 and EPIC25
644 markers. These are interpreted as evidence of "intraspecific horizontal exchange" that "can only be
645 explained by recombination between individuals". As discussed above, we calculated probabilities in
646 excess of 99% that conspecific contamination occurred sufficiently often to explain such evidence.
647 For these two trios, however, we need not even reach that hypothesis. The authors rightly note that
648 patterns of allele sharing involving closely related clones and sequences "may be explained by
649 mutations and gene conversions alone". However, they do not explicitly or quantitatively test this
650 hypothesis for either of the trios discussed before reaching their conclusions. To supply the missing
651 test, we obtained the relevant sequences for the samples comprising each trio from GenBank (Figure
652 S10). For Species A, the identities of the samples are not clear from the haplotype networks the
653 authors present in their Figure 3, but can be inferred by examining the codes in their Table S3 and
654 the sequences themselves. For the purpose of this analysis, we assume Debortoli et al. phased the
655 homologues correctly, setting aside the substantial concerns about phasing described above.
656
657 To visualise each trio explicitly, we aligned the six sequences and identified every polymorphic site
658 differentiating the three haplotypes (Figure S10). For the EPIC25 trio, Debortoli et al. state that
659 "flanking regions were sequenced...yielding five additional SNPs between haplotypes". This seems
660 to be an error, as examination of the flanking sequences reveals only two additional C/T SNPs, for a
661 total of 3 SNPs and one tandem repeat polymorphism. From each alignment, we stripped out the
662 polymorphic sites defining each haplotype, and matched them to the samples comprising the trio.
663 This gives a pair of sequences for each sample, interpreted as a single animal with two homologous
664 sequences. These were plotted to identify ways in which each trio "may be explained by mutations
665 and gene conversions alone". We began with two haplotypes from a single animal, and attempted to
666 identify the most parsimonious pathway to generate the other two clones by substitution.
667
668 For the Nu1054 trio, the simplest path identified was a single point mutation in one descendant of
669 the initial clone, and a single gene conversion event in a different descendant, with a tract length of
670 150bp (Figure S10). Evidence of both substitution events is seen commonly in other individuals from
671 the population sample. For the EPIC25 trio, the simplest hypothesis is a single point mutation in one
672 descendant of the focal clone, and a single gene conversion in another, with a tract length of 274bp
673 (Figure S10). These hypotheses are extremely parsimonious: in Species A, all but one of the Nu1054
674 and EPIC25 haplotypes (93%) are separated from a second allele by a single substitution, indicating
675 that point mutations are common and frequently persist. Gene conversion is even more common: in
676 *Adineta*, "the probability that a given base in the genome experiences gene conversion is at least

677 one order of magnitude greater than its probability to mutate" (Flot et al. 2013). The lengths of the
678 two hypothetical gene conversion events are well within the mean tract length determined in model
679 systems, including *Plasmodium*, yeast, humans and *Drosophila* (Do et al. 2014; Yim et al. 2014;
680 Williams et al. 2015; Miles et al. 2016). We therefore find that both haplotype trios in Species A
681 "may be explained by mutations and gene conversions alone", without reference to “intraspecific
682 horizontal exchange” or even to probable conspecific cross-contamination.
683
684 For completeness, we applied the same method to the EPIC25 trio in Species C (KU861135-40). The
685 600bp tract of exact allele-sharing occurs precisely at the EPIC25 marker, and ceases 100bp beyond
686 it, where the three haplotypes split into six, and undetermined bases start to interrupt the assembly.
687 At the EPIC25 marker, any pair of genotypes can be interchanged via one gene conversion (231 bp)
688 and three point mutation events (not shown), so it is not improbable for any two clones to arise "by
689 mutations and gene conversions alone". For the full trio, however, the shortest pathway requires
690 two gene conversions and six point mutations. Debortoli et al. consider this "unlikely", although that
691 assessment must be weighed against the even more extraordinary claim of “intraspecific horizontal
692 exchange”. Cross-contamination is a much more parsimonious explanation than either of these
693 alternatives, as there is a 99.98% probability that one or more Species C tubes contained DNA from
694 two rotifers. Specifically, the EPIC25 Hap6-Hap14 genotype in Sample H4-28 is found nowhere else
695 in the study, and therefore is the pairing most likely to be an artefact. As seen in Table S5, this
696 genotype will arise if a single animal homozygous for Hap6 (e.g. Individual 30) shares a tube with
697 DNA from an individual homozygous for EPIC25 Hap14, or a loose DNA fragment bearing Hap14.
698
699 We recommend that future attempts to test for recombination in presumed asexuals ought to take
700 explicit and quantitative account of alternative hypotheses for apparent allele-sharing, including
701 cross-contamination, point mutation, gene conversion, convergent substitution, natural selection,
702 phasing uncertainty, multiple gene copies, sequencing error, and the null probability of identifying
703 haplotype trios or other patterns *post-hoc*, given the numbers of isolates or genotypes examined in
704 an initial sample pool. One way to exclude these alternative hypotheses would be a direct
705 demonstration of recombination or sexual crossing between individuals or clones in the laboratory.
706
707
708
709
710

Supplemental References

1. Agresti, A. (2007). *An introduction to categorical data analysis*. 2nd edn. John Wiley & Sons, Inc., Hoboken, New Jersey

2. Barron, G. (2004). Fungal parasites and predators of rotifers, nematodes, and other invertebrates. In: *Biodiversity of fungi: inventory and monitoring methods* (eds. Mueller, G.M., Bills, G.F. & Foster, M.S.). Elsevier Academic Press, San Diego, pp. 435–450

3. Debortoli, N., Li, X., Eyres, I., Fontaneto, D., Hespeels, B., Tang, C.Q., *et al.* (2016). Genetic exchange among bdelloid rotifers is more likely due to horizontal gene transfer than to meiotic sex. *Curr. Biol.*, 26, 723–732

4. Do, A.T., Brooks, J.T., Le Neveu, M.K. & LaRocque, J.R. (2014). Double-strand break repair assays determine pathway choice and structure of gene conversion events in *Drosophila melanogaster*. *G3 Genes|Genomes|Genetics*, 4, 425–432

5. Ewing, B. & Green, P. (1998). Base-calling of automated sequencer traces using phred. II. Error probabilities. *Genome Res.*, 8, 186–194

6. Flot, J., Hespeels, B., Li, X., Noel, B., Arkhipova, I., Danchin, E.G.J., *et al.* (2013). Genomic evidence for ameiotic evolution in the bdelloid rotifer *Adineta vaga*. *Nature*, 500, 453–457

7. Folmer, O., Black, M., Hoeh, W., Lutz, R. & Vrijenhoek, R. (1994). DNA primers for amplification of mitochondrial cytochrome *c* oxidase subunit I from diverse metazoan invertebrates. *Mol. Mar. Biol. Biotechnol.*, 3, 294–299

8. Gladyshev, E. & Kleckner, N. (2016). Recombination-independent recognition of DNA homology for repeat-induced point mutation (RIP) is modulated by the underlying nucleotide sequence. *PLoS Genet.*, 12, e1006015

9. Han, T., Chang, C.-W., Kwekel, J.C., Chen, Y., Ge, Y., Martinez-Murillo, F., *et al.* (2012). Characterization of whole genome amplified (WGA) DNA for use in genotyping assay development. *BMC Genomics*, 13, 217

10. Hoff, K.J., Lange, S., Lomsadze, A., Borodovsky, M. & Stanke, M. (2015). BRAKER1: Unsupervised RNA-Seq-based genome annotation with GeneMark-ET and AUGUSTUS. *Bioinformatics*, 32, 767–769

11. Da Ines, O., Gallego, M.E. & White, C.I. (2014). Recombination-independent mechanisms and pairing of homologous chromosomes during meiosis in plants. *Mol. Plant*, 7, 492–501

12. Katoh, K., Asimenos, G. & Toh, H. (2009). Multiple alignment of DNA sequences with MAFFT. *Methods Mol. Biol.*, 537, 39–64

13. Katoh, K. & Standley, D.M. (2013). MAFFT multiple sequence alignment software version 7: Improvements in performance and usability. *Mol. Biol. Evol.*, 30, 772–780

14. Kearse, M., Moir, R., Wilson, A., Stones-Havas, S., Cheung, M., Sturrock, S., *et al.* (2012). Geneious Basic: An integrated and extendable desktop software platform for the organization and analysis of sequence data. *Bioinformatics*, 28, 1647–1649

15. Larosa, V. & Remacle, C. (2013). Transformation of the mitochondrial genome. *Int. J. Dev. Biol.*, 57, 659–665

16. Mark Welch, J.L. & Meselson, M. (1998). Karyotypes of bdelloid rotifers from three families. *Hydrobiologia*, 387, 403–407

17. McVey, M. & Lee, S.E. (2008). MMEJ repair of double-strand breaks (director's cut): deleted sequences and alternative endings. *Trends Genet.*, 24, 529–538

18. Miles, A., Iqbal, Z., Vauterin, P., Pearson, R., Campino, S., Theron, M., *et al.* (2016). Indels, structural variation, and recombination drive genomic diversity in *Plasmodium falciparum*. *Genome Res.*, 26, 1288–1299

19. Mullis, K.B., Ferre, F. & Gibbs, R.A. (1994). *The polymerase chain reaction*. Birkhäuser, Boston

20. Nei, M. & Gojobori, T. (1986). Simple methods for estimating the numbers of synonymous and nonsynonymous nucleotide substitutions. *Mol. Biol. Evol.*, 3, 418–426

21. Polz, M.F. & Cavanaugh, C.M. (1998). Bias in template-to product ratios in multitemplate PCR. *Appl. Environ. Microbiol.*, 64, 3724–3730

22. Stajich, J.E., Block, D., Boulez, K., Brenner, S.E., Chervitz, S.A., Dagdigian, C., *et al.* (2002). The Bioperl toolkit: Perl modules for the life sciences. *Genome Res.*, 12, 1611–1618

23. Thomas, C.M. & Nielsen, K.M. (2005). Mechanisms of, and barriers to, horizontal gene transfer between bacteria. *Nat. Rev. Microbiol.*, 3, 711–721

24. Vulić, M., Dionisio, F., Taddei, F. & Radman, M. (1997). Molecular keys to speciation: DNA polymorphism and the control of genetic exchange in enterobacteria. *Proc. Natl. Acad. Sci. U. S. A.*, 94, 9763–7

25. Wang, Y., Tang, H., Debarry, J.D., Tan, X., Li, J., Wang, X., *et al.* (2012). MCScanX: A toolkit for detection and evolutionary analysis of gene synteny and collinearity. *Nucleic Acids Res.*, 40, e49

26. Williams, A.L., Genovese, G., Dyer, T., Altemose, N., Truax, K., Jun, G., *et al.* (2015). Non-crossover gene conversions show strong GC bias and unexpected clustering in humans. *Elife*, 4, 1–21

27. Wilson, C.G. & Sherman, P.W. (2010). Anciently asexual bdelloid rotifers escape lethal fungal parasites by drying up and blowing away. *Science*, 327, 574–576

28. Yim, E., O'Connell, K.E., St Charles, J. & Petes, T.D. (2014). High-resolution mapping of two types of spontaneous mitotic gene conversion events in *Saccharomyces cerevisiae*. *Genetics*, 198, 181–192

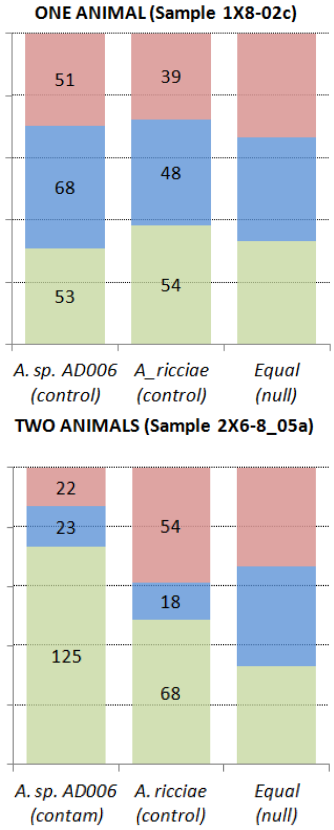

Figure S1. Minority peak analysis of mtCO1 chromatograms for two samples where *A. vaga* (AD008) was in the majority. In the first sample, *A. vaga* was the only rotifer present, and the fit of minority peaks to other haplotypes did not differ significantly from the null expectation. In the second sample, another rotifer belonging to *Adineta* sp. (AD006) was present, and minority peaks corresponding to this known contaminant were a significantly better fit than the null expectation (χ^2=123.61, d.f. = 2, P < 2.2 x 10^{-16}), or a control species, *A. ricciae* (χ^2=28.28, d.f. =2, P = 7.23 x 10^{-7}).

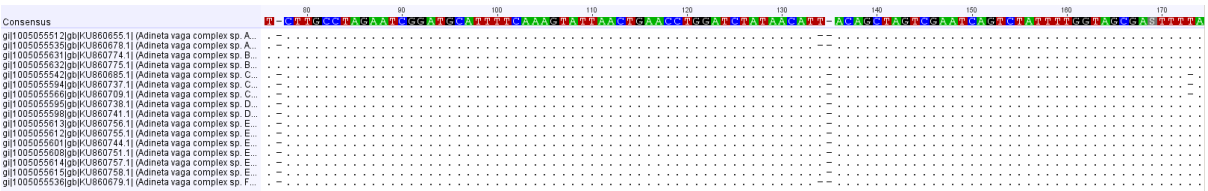

Figure S2. Insertion-deletion polymorphisms in an alignment of 28S ribosomal DNA sequences for the six *Adineta* species reported by Debortoli et al. (2016). Dots indicate agreement to the consensus sequence; dashes indicate gaps. Minority and majority sequences of different lengths are predicted to run out of phase in chromatograms for part of their length.

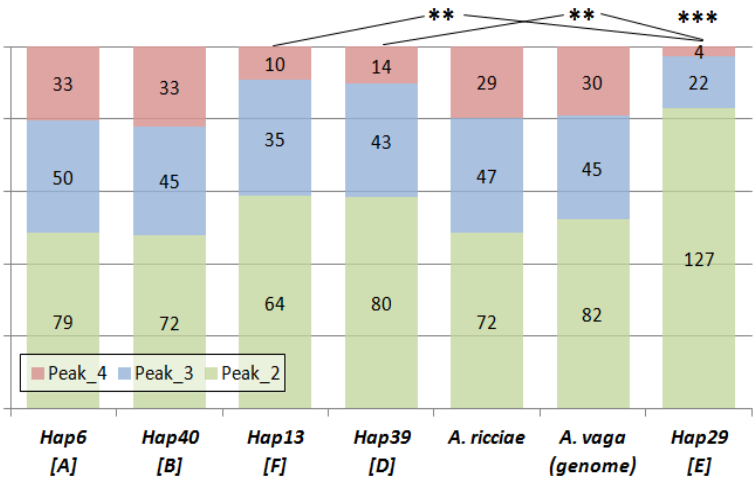

825 **Figure S3.** Summary of minority peaks in mtCO1 chromatograms for Sample B22. The fit of Hap29
826 [E] is significantly better (***) than the other six species (χ^2=69.49, d.f. = 12, P = 3.99 x 10^{-10}). If
827 Hap29 [E] is removed, the other distributions are not significantly different from one another
828 (χ^2=15.2, d.f. = 10, P = 0.124). If compared directly, Hap29 [E] is a significantly better fit (**) than
829 either Hap13 [F] (χ^2=19.48, d.f. = 2, P = 5.9 x 10^{-5}) or Hap 39 [D] (χ^2=22.2, d.f. = 2, P = 1.51 x 10^{-5}).
830

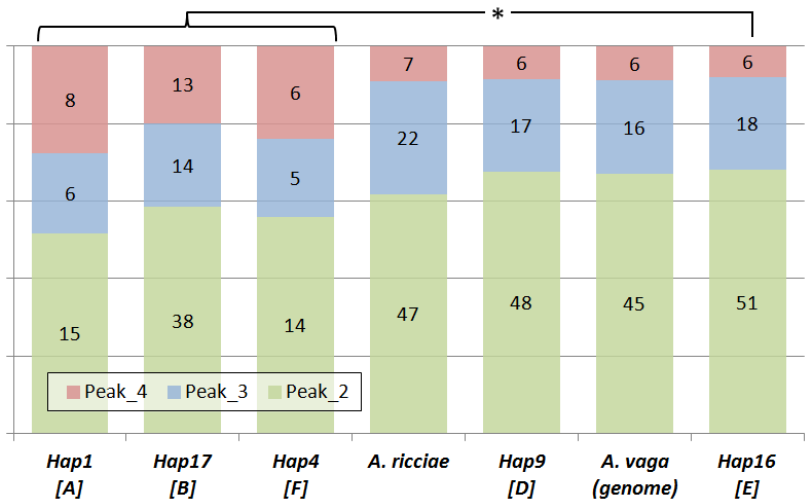

831 **Figure S4.** Summary of minority peaks in 28S chromatograms for Sample B22. Hap 16 [E] is a
832 significantly better fit to these peaks (*) than Hap1 [A], Hap 17 [B] and Hap4 [E], which were pooled
833 owing to small cell counts (χ^2=6.85, d.f. = 2, P = 0.029). The remaining species are too closely
834 related to Species E to be distinguished statistically at the conserved 28S locus.
835

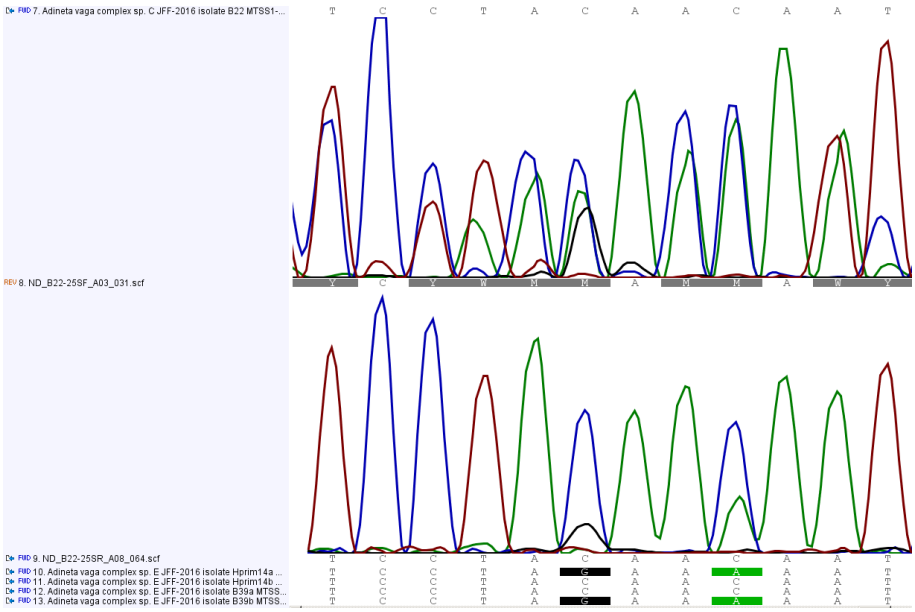

836 **Figure S5.** Shifted and double peaks in EPIC25 chromatograms for Sample B22 indicate indels and
837 SNPs between two homologous sequences, which both belong to Species E and are incongruent with
838 the Species C background. The two SNPs shown here correspond to polymorphisms seen natively in
839 "heterozygous" animals from the Species E population (Hprim14a/b and B39a/b). Horizontal import
840 of standing heterozygosity is not predicted in the model of interspecific recombination presented by
841 Debortoli et al. (2016), but it is predicted if the sequences arise from cross-contamination.
842

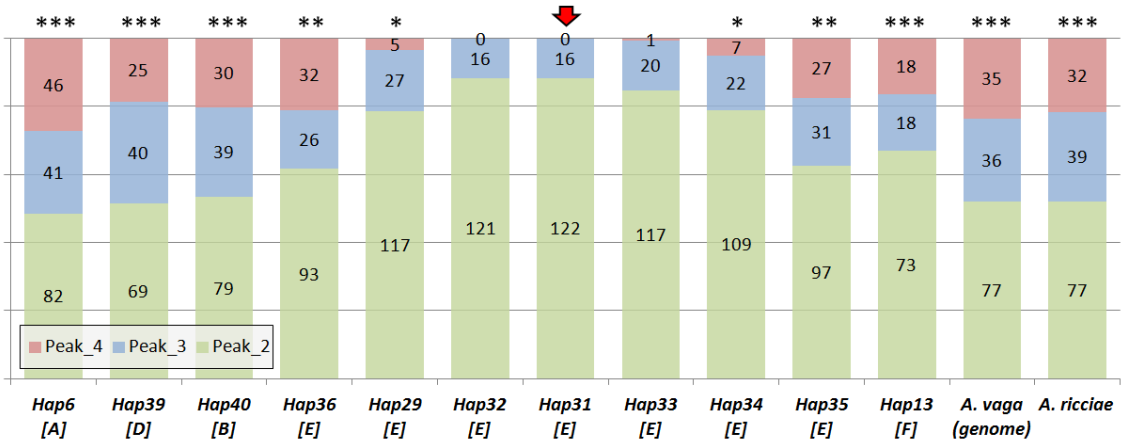

843 **Figure S6.** Minority peaks in mtCO1 chromatograms for Sample B39 (Individual 66) indicate the
844 predicted 'native' haplotype Hap31 [E] (red arrow), and challenge the hypothesis that mtDNA has
845 undergone interspecific recombination. Hap31 [E] is a significantly better match to the secondary
846 peaks than all other haplotypes (*: $\chi^2 = 9.63$, d.f. =4, P = 0.047; **: $\chi^2 = 66.71$, d.f. = 8, P = 2.21×10^{-11};
847 ***: $\chi^2 = 136$, d.f. = 20, P < 2.2×10^{-16}), except Hap32 [E] and Hap33 [E], which are nearly identical and
848 were not included in contingency table tests.

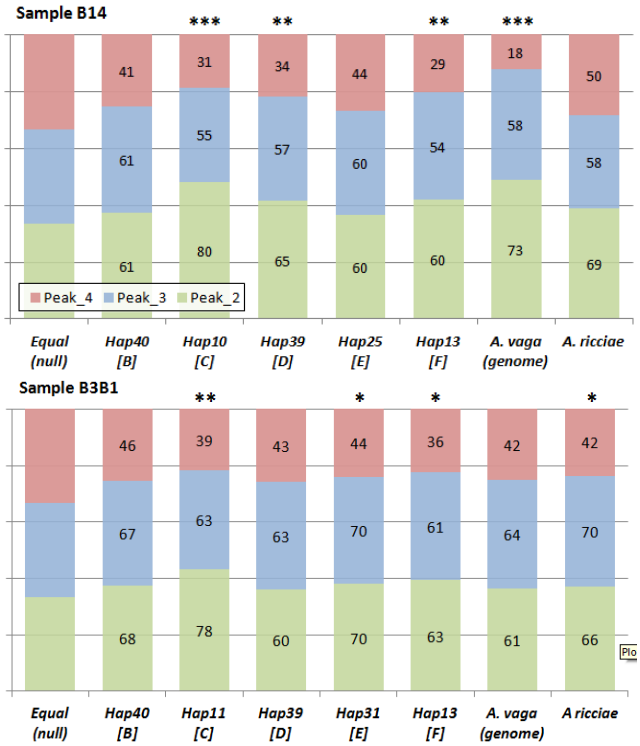

849 **Figure S7.** Analysis of minority peak distributions indicates additional mtCO1 sequences in
850 chromatograms for Samples B14 and B3B1. Multiple candidate haplotypes are a significantly better
851 fit than expected under a null distribution of peak ranks (*** : $P < 0.001$, **: $P < 0.01$; *: $P < 0.05$),
852 but their distributions do not differ significantly when compared with each other, and we cannot
853 therefore narrow down a single minority haplotype driving the pattern. This suggests two different
854 contaminating sequences are superimposed in each case, alongside the Species A majority
855 haplotype. Clear evidence for haplotypes from Species A, C and E was found at other loci.
856

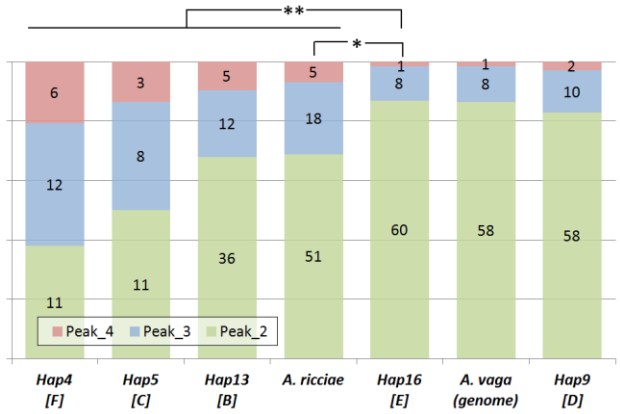

857 **Figure S8.** Minority peaks in 28S chromatograms for Sample B14 reveal a second haplotype that fits
858 Species E significantly better than Species B, C, F or *A. ricciae* (**: $\chi^2 = 28.77$, d.f. = 8, $P = 3.0 \times 10^{-4}$; * :
859 $\chi^2 = 7.1$, d.f. = 2, $P = 0.029$). Hap9 [D] and *A. vaga* (genome) are nearly identical to Hap16 [E] and
860 cannot be distinguished statistically.

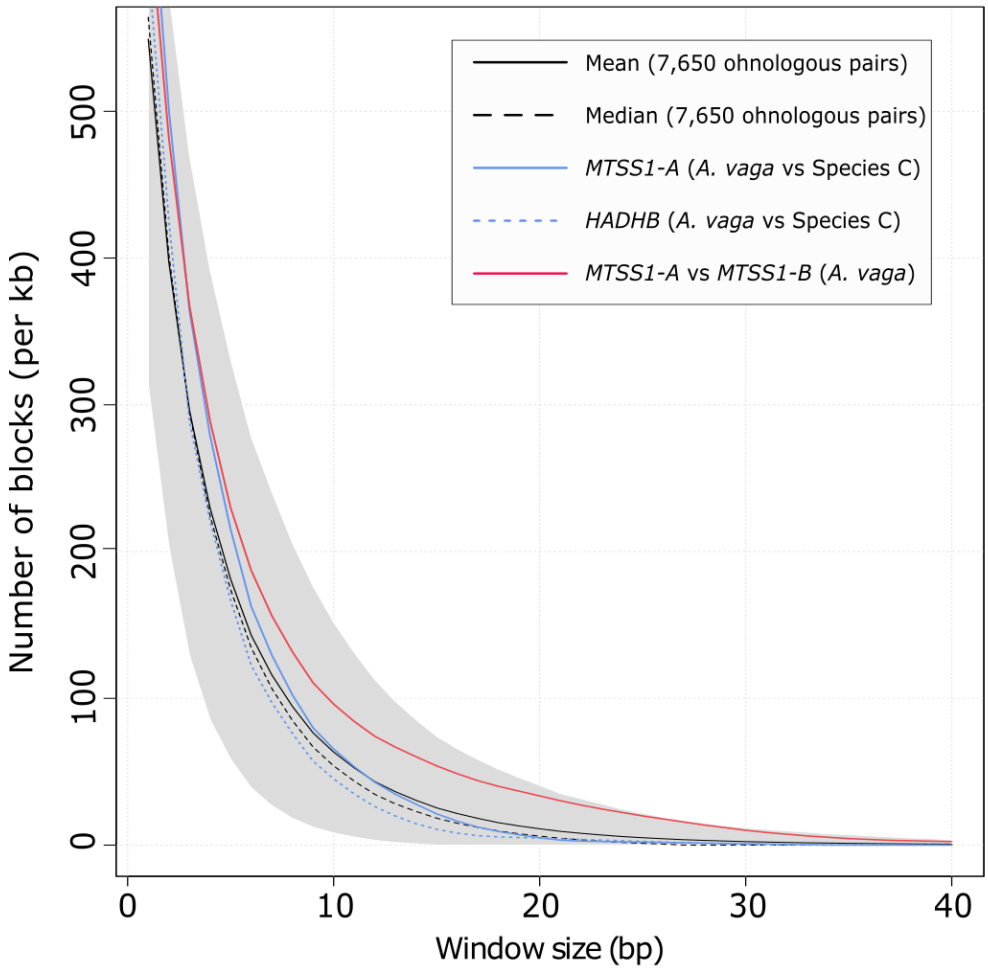

Figure S9. Two genes linked to an "interspecific horizontal genetic transfer" event did not share significantly more or longer microhomologous blocks than 7650 pairs of independently evolving ohnologous genes in the *A. vaga* reference genome. Regardless of scale (1-40bp), the degree of microhomology between "transferred" sequences (blue lines) falls within the 5% and 95% quantiles for genomic ohnologs (grey shading). The dashed blue line represents the gene *MTSS1-A*, containing the EPIC25 marker; the solid blue line shows the next-closest gene (*HADHB*). For sliding windows above 3bp, the "horizontally transferred" *MTSS1-A* sequences share less microhomology with each other than with their own independently evolving ohnolog (*MTSS1-B*) in the same genome (red line).

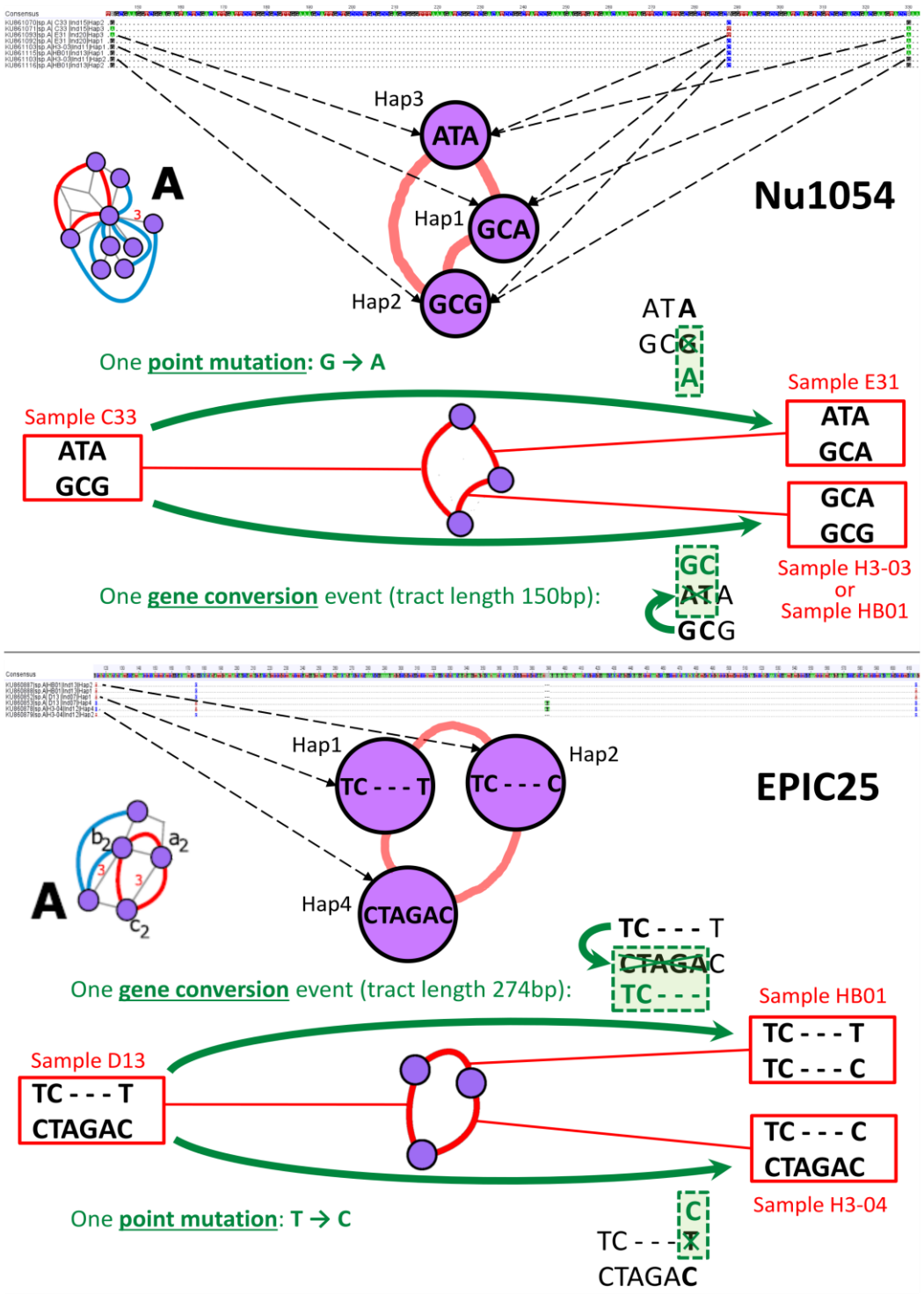

875 **Figure S10.** Debortoli et al. (2016) assert that "haplotype trios" at Nu1054 and EPIC25 "can only be
876 explained by recombination between individuals" in Species A. This figure illustrates the alternative
877 hypothesis that the trios "may be explained by mutations and gene conversions alone". All variable
878 sites are stripped from alignments of the focal sequences and mapped to haplotypes (purple circles).
879 Homologous sequence pairs are then matched to samples (in red). Both trios are parsimoniously
880 explained by one point mutation and one gene conversion arising in a single clone (green arrows).

Group name	1X6	1X8	2X6-8
Animals	One: AD006	One: AD008	Two: AD006 and AD008
Biological replicates	3	2 (1 lost)	6
Technical replicates	1 triplicate, 2 single	1 triplicate, 1 single	1 triplicate, 2 duplicate, 3 single

881

882 **Table S1.** Design and replication of an experiment to determine the effect of multiple rotifers in a
883 single DNA extraction tube. AD006: *A.* sp. 'AD006'; AD008: *A. vaga* (reference genome clone).

884

885

Sample code	Majority haplotype	Minority haplotype	Number of chromatogram files	Total bases called	Minority base calls	% sites with majority calls
01	*A.* sp. (AD006)	*A. vaga* (AD008)	2 (singleton)	1210	25	97.94
02	*A. vaga* (AD008)	*A.* sp. (AD006)	2 (singleton)	1210	5	99.59
03	*A.* sp. (AD006)	*A. vaga* (AD008)	4 (duplicated)	2420	8	99.66
04	*A. vaga* (AD008)	*A.* sp. (AD006)	2 (singleton)	1210	6	99.5
05	*A. vaga* (AD008)	*A.* sp. (AD006)	4 (duplicated)	2420	16	99.33
06	*A.* sp. (AD006)	*A. vaga* (AD008)	6 (triplicated)	3630	13	99.64

886

887 **Table S2**. Summary of base calls from ABI Sanger sequencing of mtCO1, corresponding to majority
888 and minority haplotypes for biological and technical replicates of experimentally contaminated
889 samples (Group 2X6-8). Chromatograms are always in bidirectional pairs.

890

891

Marker	Species C	Species E	C vs. E (%)	C vs. ref (%)
mtCO1	Hap10 (KU860596)	Hap29 (KU860588)	87.8	87.8
28S	Hap5 (KU860706)	Hap16 (KU860768)	97.6	97.7
EPIC25	Hap10 (KU860907)	Hap37 (KU860804)	68.4	68.4
EPIC63	Hap4 (KU860934)	Hap34 (KU860927)	67.4	67.6
Nu1054	Hap16 (KU861061)	Hap21 (KU861052)	70.1	70.2

892

893 **Table S3.** At five independent mitochondrial and nuclear marker loci, the percentage identity
894 between Species C and Species E is almost exactly reproduced by comparing Species C to the
895 reference genome of *A. vaga*. The reference genome therefore is an appropriate surrogate for
896 Species E when estimating homology parameters for a hypothetical transfer from Species C.

897

898

899

900

Comparison	Aligned length (bp)	Identity (%)
EPIC25 marker only	395	68.4
Two-gene region	8949	62.3
MTSS1 whole gene	4419	68.4
MTSS1 exons	2301	75.1
MTSS1 introns	2118	61.1
Intergenic region	2203	52.4
HADBH whole gene	2327	60.1
HADBH exons	1605	67.0
HADBH introns	722	44.7

Table S4. Pairwise identity between Species C and the *A. vaga* reference genome for the region surrounding the EPIC25 marker. Regardless of the scope or scale of the comparison, the distances are not compatible with the "interspecific recombination" claimed between Species C and Species E. The identity estimate from the short EPIC25 marker accurately reflects (or even overestimates) homology more broadly.

Number of tubes with DNA from two animals	Tube 1 genotype(s)	Tube 2 genotype(s)	Tube 3 genotype(s)
0	(a||b)	(b||c)	(c||a)
1	(a||b)	(b||c)	(c ||c) & (a||a)
1	(a||b)	(b||b) & (c||c)	(c||a)
1	(a||a) & (b||b)	(b||c)	(c||a)
2	(a||b)	(b||b) & (c||c)	(c||c) & (a||a)
2	(a||a) & (b||b)	(b||c)	(c||c) & (a||a)
2	(a||a) & (b||b)	(b||b) & (c||c)	(c||a)
3	(a||a) & (b||b)	(b||b) & (c||c)	(c||c) & (a||a)

Table S5. When tubes are contaminated with DNA from two animals of the same species, there are at least seven scenarios in which three genotypes at a focal locus (a, b, c) will be shared "in a cyclical fashion" among tubes, as reported by Debortoli et al. (2016). These scenarios explain such cycles without reference to "intraspecific horizontal exchange". As discussed for "interspecific" samples, contamination may be evident at multiple loci, and therefore presumably involves genomic DNA from two animals (e.g. Sample B11), or only at the focal locus, presumably via amplification of DNA fragments (e.g. Sample D14).

First species	P	Second species	P	P (combination)	Contamination category	Sum (P)
A	130 ÷ 547 = 0.23766	A	0.23766	0.05648	conspecific	
C	396 ÷ 547 = 0.72395	C	0.72395	0.52410	conspecific	
E	21 ÷ 547 = 0.03839	E	0.03839	0.00147	conspecific	**0.58205**
A	0.23766	C	0.72395	0.17205	heterospecific	
A	0.23766	E	0.03839	0.00912	heterospecific	
C	0.72395	A	0.23766	0.17205	heterospecific	
C	0.72395	E	0.03839	0.02779	heterospecific	
E	0.03839	A	0.23766	0.00912	heterospecific	
E	0.03839	C	0.72395	0.02779	heterospecific	**0.41795**

Table S6. Given the relative frequencies of Species A, C and E in the material sampled by Debortoli et al. (2016), 0.418 of all cross-contaminated tubes are expected to contain DNA from heterospecific animals, and 0.582 will contain DNA from conspecific animals. Because heterospecific contamination is found in 6 of 72 tubes, the number expected to show conspecific contamination is 6 x 0.582 ÷ (1 - 0.582) = 8.36 ≈ 8. The total expected rate of contamination *t* is (8.36 + 6) ÷ 72 = 0.199 (14 tubes), but this will be dramatically higher if pairs of animals drawn from the same patch are more likely to belong to the same rather than different species, as demonstrated empirically by Debortoli et al.